Desalination and Water Treatment
www.deswater.com
doi: 10.5004/dwt.2021.26495

209 (2021) 379–391
January

Box–Behnken experimental design for the optimization of Basic Violet 03 dye removal by groundnut shell derived biochar

Josephraj Jegan[a], Saravanan Praveen[a,*], Balasubramanian Muthu Kumar[b], Thillainayagam Bhagavathi Pushpa[a,*], Ravindiran Gokulan[c]

[a]*Department of Civil Engineering, Anna University, University College of Engineering Ramanathapuram, Ramanathapuram 623 513, Tamil Nadu, India, emails: praveensarvan@gmail.com (S. Praveen), pushpathillai@gmail.com (T. Bhagavathi Pushpa), drjeganjoe@gmail.com (J. Jegan)*
[b]*Department of Computer Science and Engineering, Syed Ammal Engineering College, Ramanathapuram 623 502, Tamil Nadu, India, email: muthu122@gmail.com (B. Muthu Kumar)*
[c]*Department of Civil Engineering, GMR Institute of Technology, Rajam, Srikakulam 532 127, Andhra Pradesh, India, email: gokulravi4455@gmail.com (R. Gokulan)*

Received 4 April 2020; Accepted 25 August 2020

ABSTRACT

The current experimental work was designed to explore the maximum biosorption efficiency of biochar derived from agricultural waste groundnut shell (GnSB) for the removal of Basic Violet 03 (BV03) dye from aqueous solution. To validate and optimize interactions among different parameters (pH, biochar dosage, temperature, initial dye concentration and contact time) for the removal of BV03 in aqueous solution, the Box–Behnken design (BBD) model of response surface methodology was employed. Forty-six base run was carried out with six center points. The values of *F* and *P* obtained from this design revealed that the BBD model was suitable for analyzing the effects of interaction among different parameters. Pareto analysis has been used to found the most influential process condition as biochar dose. The optimum conditions were found to be 42°C of temperature, 6 g L^{-1} of biochar dosage, 60 min of contact time at a concentration of 50 mg L^{-1} and pH 7. The study confirms that 96.56% of dye removal was obtained in the optimized condition.

Keywords: Biochar; Groundnut; Basic Violet 03; Response surface methodology

1. Introduction

Life in the modern world faces many challenges with substantial changes in the climate due to excessive industrial and individual activities. Textile industries are also one of the major root causes of environmental pollutions, due to its huge amount of toxic dye-contaminated wastewater generation [1]. The usage of synthetic dyes in these industries led to an increase in the pollution level in the existing system and it should be treated before these wastewaters being discharged into the ecosystem [2].

However, a limited number of textile industries are using various treatment techniques such as biodegradation, membrane separation, coagulation and flocculation, oxidation and ozonation, photocatalytic degradation, and electrochemical degradation [3–5]. Yet, these methods have certain limitations such as the formation of hazardous by-products, deficiency of eco-friendliness, energy consumptions, and high operating cost [6].

Biological processes such as biosorption [7], bioaccumulation [8], and biodegradation [9] having greater potential applications in the removal of dyes from textile wastewater.

* Corresponding authors.

Therefore, an alternate eco-friendly treatment technique is needed. Biological-adsorption can be defined as the uptake of pollutants by inactive biomass through physiochemical treatments [10]. Biosorption is an innovative process, which consumes dead biomass for dye removal. The use of lignocellulosic biomass [11] provides the benefits of higher biosorption, with more economic, extensive accessibility, and repeated utilization of biomass [12]. Biomass-derived from different agricultural waste will be a cost-effective and eco-friendly solution for dye removal from wastewater [13,14]. The waste residues of agricultural industries would be the good alternate, cheap, and highly available resources without the expensive cost of processing, instead of using activated carbon [15]. Groundnut shell is lignocellulosic biomass obtained as a waste residue from the groundnut processing units [16] will be used as dead biomass for the biosorption techniques and this bio-based raw material have been converted as biochar through thermochemical conversion in a limited oxygen environment [17] will be used as a sorbent in the biosorption process.

Biochar is a complex carbonaceous material with numerous physical and chemical parameters that control its reactivity in aqueous solution to inorganic and organic species [18]. Today, many environmental remediation studies have focused on biochar and biochar-based adsorbents [19]. Since when compared to raw adsorbents, biochar produced from the feedstock will increase the adsorption capacity by increasing the binding sites and surface area. After adsorption of dye, biochar can also be regenerated for the further adsorption process [20].

In this context, the experimental investigation was carried out to define the viability of the ecofriendly application of groundnut shell derived biochar (GnSB) in the remediation of Basic Violet 03 (BV03) from aqueous solution. To the best of our knowledge, GnSB has not been previously investigated for the removal of BV03 from the aqueous solution. Further, the effect of parameters such as the solution pH, biochar dosage, temperature, contact time, and initial dye concentration on the biosorption capacity of GnSB was evaluated.

To further investigate the effect of various operational parameters, response surface methodology (RSM) was carried out based on the concept of design of experiments (DoE). DoE is a significant technique because it provides a statistical model that helps in optimizing different operational parameters and their interactions [21]. Besides, it requires only a minimum number of experiments, low time consumption, minimizes the amount of various resource requirements [22]. Therefore, this investigation is focused on the statistical optimization of operational parameter conditions for the sorption of BV03 from GnSB. Statistical optimization was further carried out to determine the optimum conditions for the adsorption of BV03.

2. Materials and methods

2.1. Biomass and chemicals

An agricultural waste by-product of groundnut shell was used in the present investigation. These waste residues of groundnut shells are collected from groundnut oil agro-processing units in Coimbatore, Tamilnadu, India. The collected groundnut shells were used as the feedstock for biochar preparation. These feedstocks were initially washed up with tap water to remove soil with dust and then exposed to natural drying for 48 h. Now all the feedstocks were further dried up to at 70°C for 24 h, and then pulverized to less than 100 mm for biochar production [23]. BV03 with a molecular weight of 407.98 g mol^{-1} and all other chemicals used in this experiment was acquired from Sigma-Aldrich India Pvt. Ltd. The chemical structure of BV03 is shown in Fig. 1.

2.2. Pyrolysis of biomass

The measured amount groundnut shell of 100 g was kept in a closed crucible covered with small holes of alumina foil and then flamed at a preferred temperature in a muffle furnace [24] and maintained it for 2 h in the same operating conditions under a limited oxygen environment. The temperature routine was maintained at 5°C min^{-1}. Once after the completion of pyrolysis, the resultant biochar was further allowed to cool for room temperature overnight. This experiment was performed at different temperatures (300°C, 350°C, 400°C, 450°C, and 500°C) with three trails at each condition. The resultant biochar was moved to a desiccator and further used for various sorption studies. The adsorption performance of the biochar is highly dependent on the pyrolytic temperature and chemical composition of the feedstock used [25].

2.3. Characterization of biochar

The scanning electron microscopy (SEM) was used to analyze the surface physical morphologies of groundnut shell biochar samples. SEM analysis of biochar samples was performed using a (ZEISS-Gemini SEM) scanning electron microscope. Before analysis, all dried biochar samples were coated with a thin layer of gold for electrical conduction. A Fourier-transform infrared (FTIR) spectrophotometer (Thermo Scientific Ltd., USA, and Nicolet 6700) has been used to examine the availability of different surface functional groups on different biochars. Before these analyses, these dried samples were assorted with KBr to form pellets. The FTIR spectrum could help to depict the possible variations in the abundance of surface functional moieties of biomass in comparison with produced biochar [26]. The surface characteristics of the sample were determined by using surface area and pore size analyzer (BELSORP mini II) on nitrogen adsorption at 77 K.

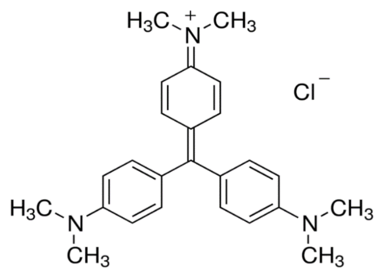

Fig. 1. Chemical structure of Basic Violet 03.

2.4. Batch adsorption process

In order to achieve the maximum uptake capacity and to optimize the operating parameters, the batch experiment trials were performed. The biochar dose was conveyed to a 250 mL Erlenmeyer flask consist of 100 mL of desired BV03 concentration and it was mixed well using an incubated shaker at 200 rpm for 6 h. Then the solution was centrifuged for 10 min at 2,500 rpm. Finally, the dye concentration was measured using a spectrophotometer from the supernatant. The effect of pH characteristic was also confirmed by the point of zero charge (pHpzc) of GnSB, which was determined by a solid addition method [27]. These adsorption trials have been continued for different process conditions.

2.5. Kinetic study

The kinetic study is important for the adsorption process because not only it describes the uptake rate of adsorbate, but it controls also the residual time of the whole process. The experiments are carried out based on the design matrix, different output variables as experimental values are put in a design matrix to find out the optimum process conditions. Also, the adequacy of the models was justified by the study of the analysis of variance.

2.6. Elution and regeneration

The desorption of dye-bounded GnSB was analyzed using various elutants, such as 0.01 M HCl, 0.01 M HNO_3, 0.01 M H_2SO_4, 0.01 M NaOH, and 0.01 M $CaCl_2$. The sorption–elution process was repeated to determine the regenerating efficiency of the sorbent.

2.7. Design of experiment

DoE is an approach to identify the relationship between cause and effect. The objective of the statistical design of experiments is to obtain the maximum source of related information with minimum resources, however, it should be as simple as consistent with the requirements of the problem. Box–Behnken design (BBD) of experiments are used to determine the effect of various influencing factors such as pH, temperature, biochar dose, initial concentration of dye, and contact time. Literature indicates that the importance of using BBD and it is found to be very effective for optimizing the adsorption influencing factors. This method represents a box where in each factor is varied at three levels–midpoints of the edges and at the center as –1, 0, and +1 indicating low, medium, and high values [28] as shown in Fig. 2. For 5 independent operating parameters, 6 center-points and 46 base runs were required to build the box. As each sample was in replicate, the total number of runs required for the analysis was 46. The optimization of variables and their interaction was carried out using the main effect, interaction, Pareto charts, surface, and contour plots. The regression analysis and design of experiments were done by using Minitab 18 software. Table 1 shows the BBD with actual and coded values of the variables. The BBD was analyzed using a quadratic equation as shown in Eq. (1). In order to evaluate the accuracy of the model, Pareto analysis of variance (ANOVA) [29] tests were performed.

$$Y = \beta_0 + \sum_{i=1}^{k}\beta_i x_i + \sum_{i=1}^{K}\beta_{ii} x_i^2 + \sum_{i=1} 0 \sum_{j=i+1}\left(\beta_{ij} x_i x_{ij} + \in\right) \quad (1)$$

where Y is the response (% Removal), β is the regression coefficient. Where x_i and x_j are independent variables and ε is the error.

3. Results and discussion

3.1. Biochar characterization

The SEM was used to assess the surface morphological functionalities of biochars produced from groundnut shell and the biochar bounded with BV03 as shown in Fig. 3 From this, it is apparent that the raw groundnut shell surface is observed as smooth. But after thermal decomposition, the adsorbent surface is found to be rough and it will enlarge the surface sites of the adsorbent and attain more binding action between BV03 to the biochar. The considerable variations were found on the surface of the biochar after bounded by BV03, which revealed that the ion exchange between the adsorbent took place [30]. In the energy-dispersive X-ray spectroscopy (EDX) analysis, strong peaks of C, N, O and S have observed for groundnut shell derived biochar as shown in Fig. 4 [30]. In the previous research of this experiment [31] was found that, the carbon and nitrogen content increases and whereas oxygen and sulfur content

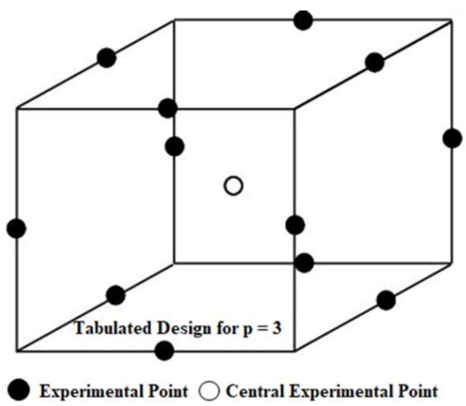

Fig. 2. Distribution of design points for Box–Behnken design.

Table 1
Values of independent variables at different levels of Box–Behnken design

Independent variables	Levels		
	–1	0	1
pH	7	8	9
Temperature, °C	35	40	45
Biochar dose, g	0.2	0.4	0.6
Initial dye concentration, mg L^{-1}	50	75	100
Contact time, min	60	90	120

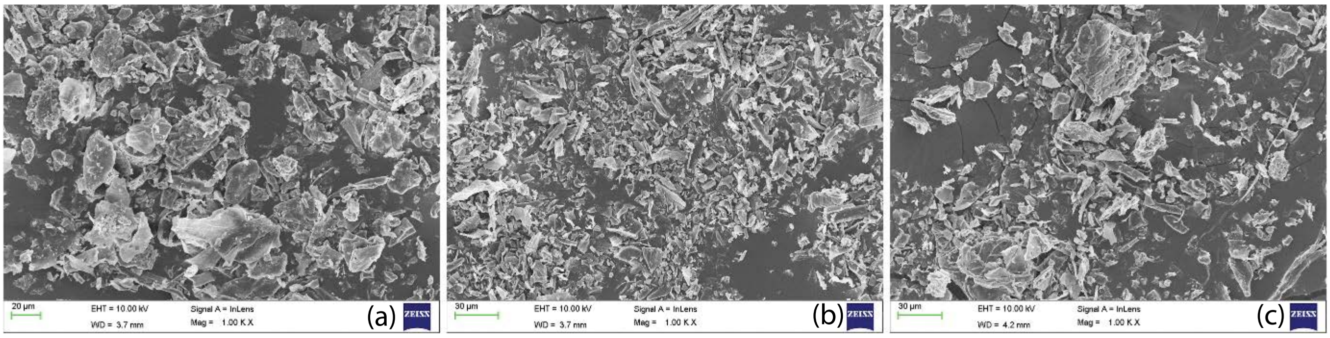

Fig. 3. SEM images of (a) groundnut shell, (b) groundnut shell derived biochar and (c) BV03 bounded groundnut shell derived biochar.

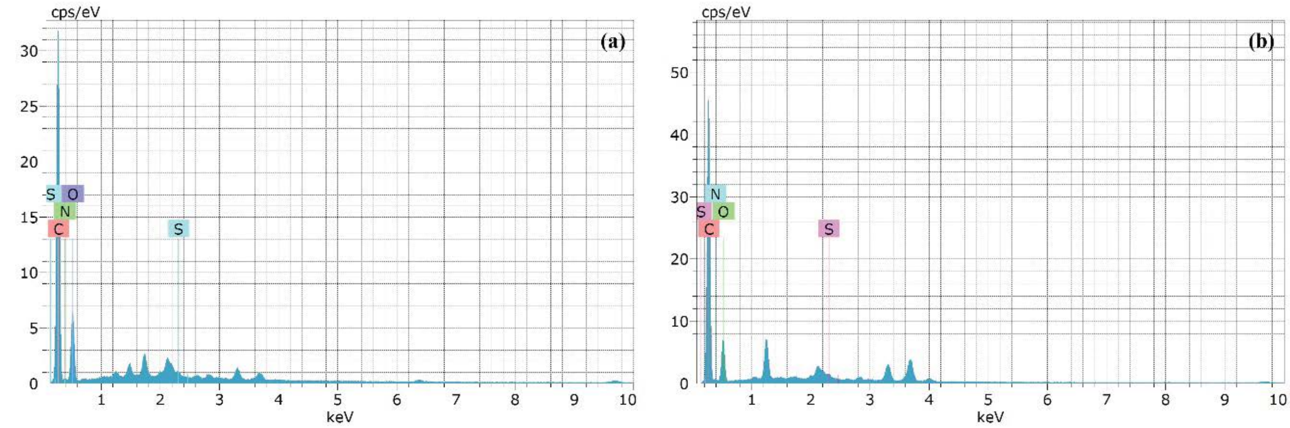

Fig. 4. (a) EDX spectrum of groundnut shell and (b) groundnut shell derived biochar.

decreases after pyrolysis. The surface area (2.34 $m^2 g^{-1}$) of the GnSB was determined by N_2 adsorption at 77 K, with the Brunauer–Emmett–Teller (BET) technique using a surface area analyzer and calculated the mean pore diameter (26.67 nm) and total pore volume (1.56 $cm^3 g^{-1}$) using the same. The condensation of organic volatiles after pyrolysis may also clog pores and results in lower BET surface areas. SEM images of GnSB seem to support this inference and it shows condensate like residue that appears to clog the pores.

Fig. 5 shows the FTIR spectrum of groundnut shell derived biochar and BV03 bounded biochar. The spectrum shows several peaks, which indicates the complex nature of the biochars. The FTIR spectrum of biochar pointed out the presence of strong bands at 613 cm^{-1} (C–H (alkenes) band), 1,172 cm^{-1} (C–O stretch (primary alcohol), 1,582 cm^{-1} (C=C stretch, N–H bend) and 3,210 cm^{-1} (O–H, N–H, stretch). From the FTIR spectrum, it was cleared that the biochar bounded with BV03 revealed the shifts in the functional group and it's due to the transformation of various ions existent in the active sites of the surface of the adsorbent by BV03 sorption. Consequently, the data obtained from the FTIR spectrum reveals the involvement of numerous functional groups such as the carboxyl and hydroxyl groups on the biochar matrix indicates that all these could have the prospect to be used as an amendment of soil for improving the cation exchange capacity and as a probable adsorbent [32]. Table 2 shows the FTIR spectra observed data of biochar samples and sorption towards the BV03 inspected.

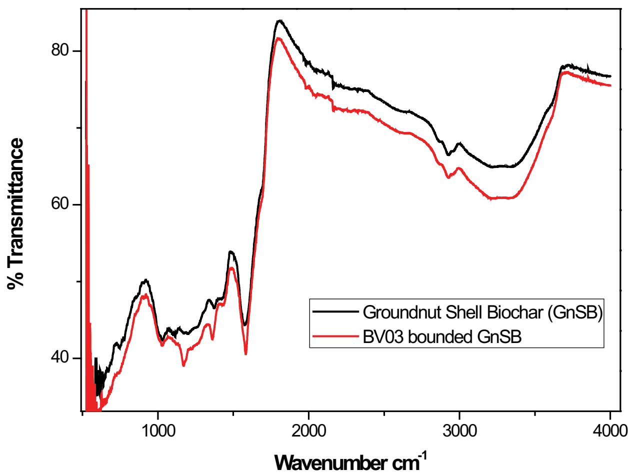

Fig. 5. FTIR spectrum of GnSB and BV03 bounded GnSB.

3.2. Adsorption isotherm and kinetics

The experimental study about the adsorption isotherm and kinetics were studied earlier as referred by Jegan et al. [31]. The applicability of the isotherm equation is compared by adjudicating the correlation coefficient value (R^2). The two-parameter models of Langmuir and Freundlich isotherms and three-parameter models of Sips and Toth isotherms were evaluated and plotted for the BV03 dye with GnSB. Out of all examined models, Toth model was found to have maximum adsorption capacity (Q_{max} of 95.07 mg g^{-1}). Kinetic models of pseudo-first-order and pseudo-second-order were applied to the experimental data to find the best fit model for the sorption process. It was observed that biosorption of BV03 on to GnSB was a swift process with maximum biosorption occurred within a few hours of the contact followed by slow attainment of equilibrium. By the application of kinetics data, it can be inferred that the pseudo-first-order kinetics is marginally superior to the second-order model. As the calculated q_e values from the pseudo-second-order kinetic model were not in good agreement with the experimental q_e values.

Table 2
FTIR spectra stretching frequencies in BV03 bounded GnSB

Assignment	Wavenumber (cm^{-1})	
	GnSB	BV03 bounded GnSB
C–H bend (alkenes)	613	614
C–O stretch (primary alcohol)	1,027	1,172
C=C stretch, N–H bend	1,574	1,582
O–H, N–H, stretch	3,219	3,210

3.3. Empirical modeling

The design matrix of the coded and real values for the adsorption of BV03 from the GnSB are given in Table 3. The results obtained from the design matrix were used to evaluate the relationship between pH (A), temperature (B), biochar dose (C), initial concentration (D) and contact time (E). The equation developed and an interactive regression model are shown in Eq. (2).

$$\begin{aligned}\%\text{ of Removal} = {} & 41.4 + 6.06A + 1.170B + 32.30C + 0.0004D + 0.0395E - 0.4475A^2 - 0.01303B^2 - 19.29C^2 - 0.000292D^2 + \\ & 0.000141E^2 + 0.0079AB - 0.925AC + 0.00268AD + 0.00387AE - 0.022BC - 0.000068BD - 0.001923BE + \\ & 0.0065CD - 0.0358CE - 0.000130DE \end{aligned} \quad (2)$$

Fig. 6 shows calculated results using Eq. (2) against the experimental results. It is clear from the graph that the regression equations follow the experimental results with

Table 3
ANOVA for percentage dye removal

Source	DF	Adj. SS	Adj. MS	*F*	*P*
Model	20	47.7145	2.3857	55.46	0.000
Linear	**5**	**39.5367**	**7.9073**	**183.81**	**0.000**
pH	1	5.8217	5.8217	135.33	0.000
Temperature	1	0.0035	0.0035	0.08	0.777
Biochar dose	1	21.8813	21.8813	508.64	0.000
Initial concentration	1	11.4256	11.4256	265.59	0.000
Contact time	1	0.4045	0.4045	9.40	0.005
Square	**5**	**7.4007**	**1.4801**	**34.41**	**0.000**
pH × pH	1	1.7473	1.7473	40.62	0.000
Temperature × temperature	1	0.9260	0.9260	21.53	0.000
Biochar dose × biochar dose	1	5.1947	5.1947	120.75	0.000
Initial concentration × initial concentration	1	0.2905	0.2905	6.75	0.015
Contact time × contact time	1	0.1399	0.1399	3.25	0.083
2-Way interaction	**10**	**0.7771**	**0.0777**	**1.81**	**0.112**
pH × temperature	1	0.0062	0.0062	0.14	0.708
pH × biochar dose	1	0.1368	0.1368	3.18	0.087
pH × initial concentration	1	0.0179	0.0179	0.42	0.525
pH × contact time	1	0.0538	0.0538	1.25	0.274
Temperature × biochar dose	1	0.0020	0.0020	0.05	0.831
Temperature × initial concentration	1	0.0003	0.0003	0.01	0.935
Temperature × contact time	1	0.3329	0.3329	7.74	0.010
Biochar dose × initial concentration	1	0.0043	0.0043	0.10	0.755
Biochar dose × contact time	1	0.1849	0.1849	4.30	0.049
Initial concentration × contact time	1	0.0380	0.0380	0.88	0.356
Error	**25**	**1.0755**	**0.0430**		
Lack-of-fit	20	1.0501	0.0525	10.33	0.008
Pure error	5	0.0254	0.0051		
Total	**45**	**48.7900**			

good accuracy (R^2 = 0.9788) and Fig. 7 shows the residual plots for the dye removal efficiency.

3.4. Analysis of variance study

The analysis of variance (ANOVA) is used to determine the significant variables. ANOVA consists of classifying and cross classifying statistical results and tested by the means of a specified classification difference, which was carried out by Fisher's statistical test (*F*-test). The *F*-value represents the significance of each controlled variable on the tested model. The correlation coefficient values R^2 and R^2_{adj} have been calculated to check the adequacy of the model. The significance of the coefficient was determined by *t*-test and *p*-values. The *t*-value represents the ratio of the estimated parameter effect to the estimated parameter standard deviation. Moreover, the *p*-value is used to check the significance of each coefficient. The larger magnitude of the *t*-value and the smaller *p*-value, the more significant is the corresponding parameter in the regression model. The results showed the highest influence was exerted by the biochar dose on the adsorption condition. Moreover, the *p*-value (0.008), which is less than 0.05, shows the significance of the model. This lack of fit can be eliminated by increasing the degree of freedom. Similar results were observed by [33]. The results of ANOVA studies are given in Table 3.

3.5. Pareto charts

The relative importance of the main effects and interaction effects can be determined through the Pareto chart as shown in Fig. 8. This analysis calculates the effect of each factor. A student's *t*-test was performed to determine whether the calculated effects were significantly different from zero, these values for each effect are shown in the Pareto chart by horizontal columns [34]. For 45° of freedom and a 95% confidence level, the *t*-value was 2.06. The values that were exceeding the reference line were significant with confidence level whereas the values before the reference line were not significant. As shown in Fig. 8, the main factors such as biochar dose (*C*), initial concentration (*D*), pH (*A*) and the interaction of biochar dose-biochar dose (CC) were found to be more significant at the 0.05 level. Whereas temperature–concentration (BD) and temperature – biochar dose (BC) had a negligible effect and were not significant

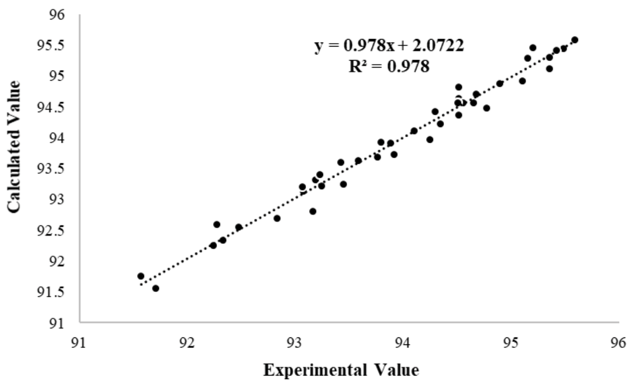

Fig. 6. Predicted vs. experimental values for the removal of BV03.

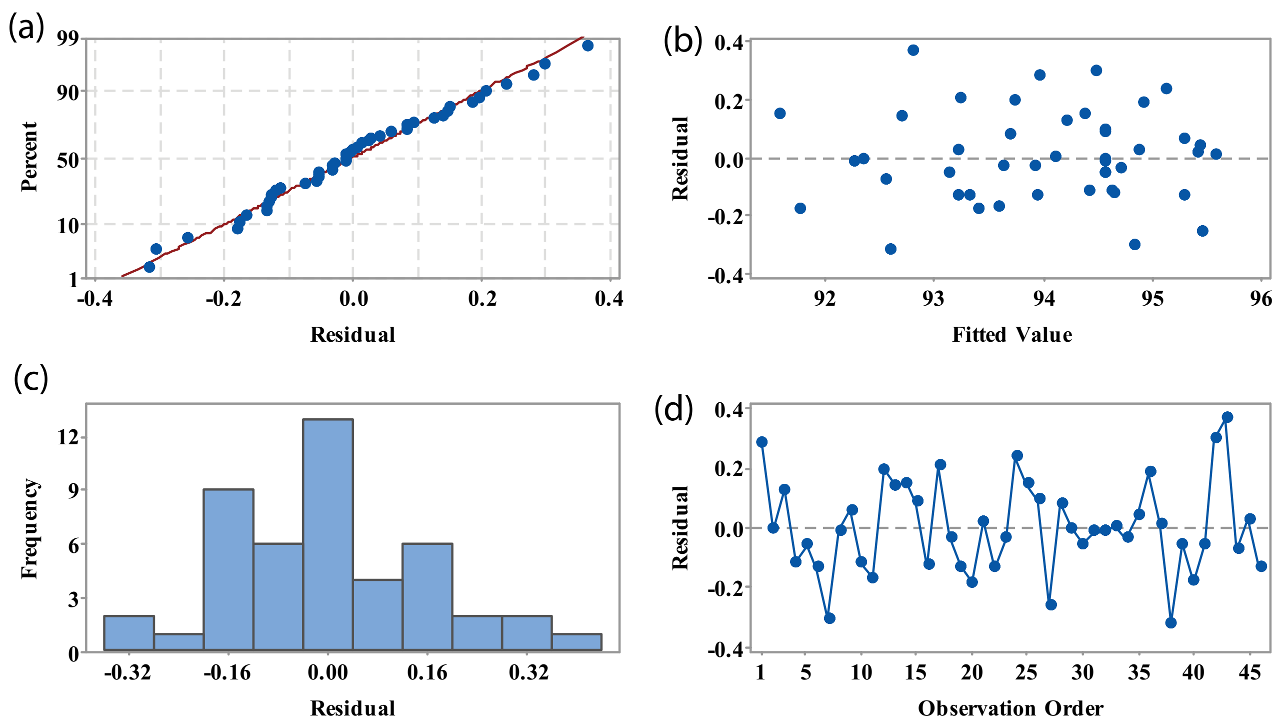

Fig. 7. Residual plots for % removal were predicted. (a) Normal probability plot, (b) versus fits, (c) histogram, and (d) versus order.

Table 4
BBD matrix for process parameters with experiment and RSM predicted % removal of BV03

Run order	Process parameters					% Removal		Error
	pH	Temperature	Biochar dose	Initial dye concentration	Contact time	Experiment	RSM	RSM
1	8	40	0.6	100	90	94.25	93.964	0.28
2	8	45	0.2	75	90	92.33	92.331	0.00
3	8	35	0.4	75	60	94.34	94.217	0.13
4	7	35	0.4	75	90	94.30	94.415	–0.12
5	9	35	0.4	75	90	93.07	93.130	–0.06
6	8	45	0.4	75	120	93.80	93.929	–0.13
7	8	45	0.4	75	60	94.52	94.824	–0.31
8	8	40	0.4	75	90	94.55	94.561	–0.01
9	7	40	0.6	75	90	95.36	95.299	0.06
10	8	45	0.6	75	90	94.51	94.626	–0.12
11	9	40	0.4	75	120	93.43	93.594	–0.17
12	9	40	0.6	75	90	93.92	93.723	0.20
13	8	40	0.2	75	60	92.83	92.690	0.14
14	7	45	0.4	75	90	94.52	94.366	0.15
15	8	40	0.4	75	90	94.65	94.561	0.08
16	8	35	0.6	75	90	94.51	94.640	–0.13
17	9	45	0.4	75	90	93.45	93.239	0.21
18	8	40	0.4	100	60	93.89	93.916	–0.03
19	8	40	0.2	50	90	93.19	93.315	–0.13
20	9	40	0.2	75	90	91.57	91.754	–0.18
21	8	35	0.4	50	90	94.90	94.874	0.02
22	8	40	0.4	50	120	95.16	95.289	–0.13
23	8	40	0.6	75	120	94.68	94.711	–0.04
24	7	40	0.4	75	60	95.36	95.118	0.24
25	8	40	0.2	100	90	91.71	91.560	0.15
26	8	40	0.4	75	90	94.66	94.561	0.09
27	8	40	0.6	75	60	95.20	95.459	–0.26
28	9	40	0.4	75	60	93.76	93.680	0.08
29	9	40	0.4	50	90	94.11	94.106	0.00
30	8	40	0.4	75	90	94.51	94.561	–0.06
31	7	40	0.4	75	120	94.56	94.568	–0.01
32	8	35	0.2	75	90	92.25	92.257	–0.01
33	8	40	0.6	50	90	95.59	95.589	0.01
34	7	40	0.4	100	90	93.59	93.622	–0.03
35	7	40	0.4	50	90	95.49	95.446	0.04
36	8	45	0.4	50	90	95.11	94.921	0.18
37	8	40	0.4	50	60	95.43	95.412	0.01
38	7	40	0.2	75	90	92.27	92.591	–0.32
39	8	40	0.4	75	90	94.51	94.561	–0.06
40	8	40	0.4	100	120	93.23	93.403	–0.18
41	8	40	0.4	75	90	94.51	94.561	–0.06
42	8	35	0.4	75	120	94.78	94.476	0.30
43	8	40	0.2	75	120	93.17	92.802	0.36
44	9	40	0.4	100	90	92.48	92.550	–0.07
45	8	45	0.4	100	90	93.24	93.214	0.03
46	8	35	0.4	100	90	93.07	93.201	–0.13

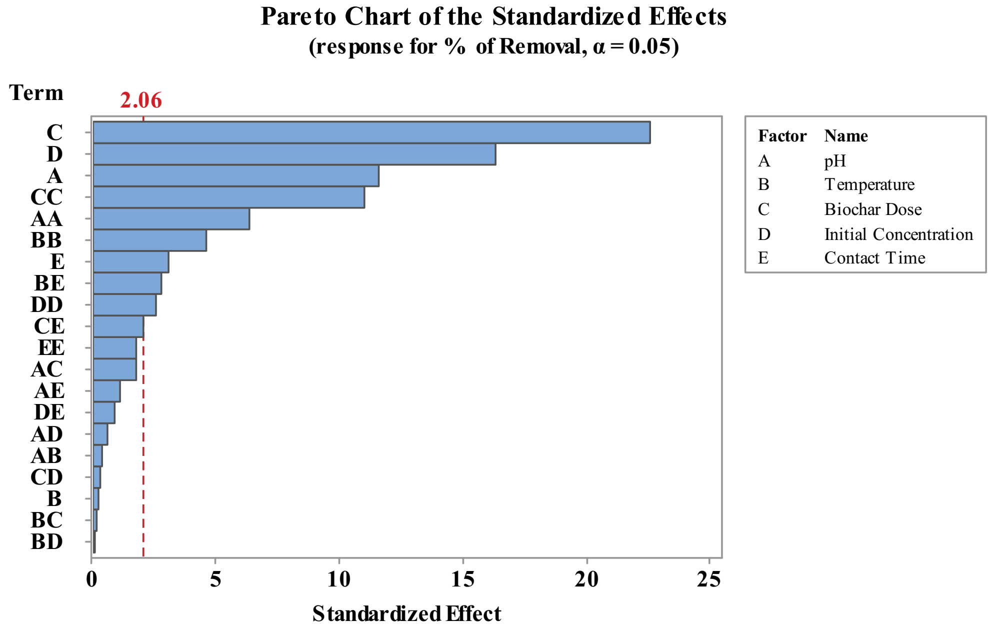

Fig. 8. Pareto graph for BV03 dye removal.

for sorption of BV03 from the adsorbent ground nutshell derived biochar [35].

3.6. Response surface analysis

The surface and contour plots for the adsorption of BV03 from the biochar derived from groundnut shell are shown in Figs. 9–11 and all these plots are generated by keeping any one factor at the optimum condition and varying other factors to study their main and interaction effect. It was clearly observed from the figures that the dye removal is favorable with a high biochar dose. Similar results have been noted by [36,37]. But while the initial dye concentration increases upto 60 mg L^{-1}, at pH 7, in the early hours of adsorption results in increases the % removal. Figs. 9–11 explore the effects of process parameters that can be influenced by the adsorption process. As the pH of the adsorbate solution decreases the adsorbent surface becomes more and more acid which in turn and enhances the electrostatic force of attraction between the anionic adsorbent surface and the cationic dye molecules lead to higher removal percentage. A three-dimensional response surface was used to examine the interaction strength between any two process parameters on the influence of the removal rate of BV03 and kept another process condition was considered as a central point. The response surface analysis revealed that the interaction of high biochar dose with other parameters exhibits better removal of BV03.

3.7. Optimization of parametric condition

Fig. 12 shows the graphical representation of numerical optimization. This figure advocates that pH value should be kept as low as possible, as dye removal increases monotonically with decreasing pH. The optimum values of pH, temperature, biochar dose, initial dye concentration and time are obtained as 7, 42°C, 6 g L^{-1}, 50 mg L^{-1} and 60 min respectively. The maximum dye removal at this optimum condition was 96.60%.

3.8. Comparison between experimental and RSM predictive model

The predicted response and error of RSM with experimental data are summarized in Table 4 and it is evident from the table that most of the observations, the error is <0.30, that shows the predicted response by RSM is in good agreement with the experimental removal efficiency.

4. Conclusion

The adsorption of BV03 dye was performed by using groundnut shell derived biochar with a maximum removal efficiency of 92.20% at the process conditions of biochar dosage of 4 g L^{-1}, pH of 8, the temperature of 40°C and initial dye concentration of 75 mg L^{-1}. Whereas the statistical optimization of all these parameters was also performed with techniques of regression. The statistical analysis confirmed that the pH, temperature, biochar dose, initial dye concentration and contact time had an individual effect on the adsorption of BV03. In addition, there will be a significant interaction between temperature and contact time. The characterization of biochar and BV03 bounded biochar shows a shift in their functional group and its shows the presence of C, N, O and S. The Box–Behnken design experiment of RSM is compared with the experimental trials and response surface Box–Behnken design is found to be the best fit model with a correlation coefficient (R^2) of 0.978. From the response optimizer, the optimized process conditions are biochar dosage (6 g L^{-1}), pH (7), temperature (42°C), initial dye concentration (50 mg L^{-1}) at a contact time of 60 min with a maximum predicted removal of 96.56%.

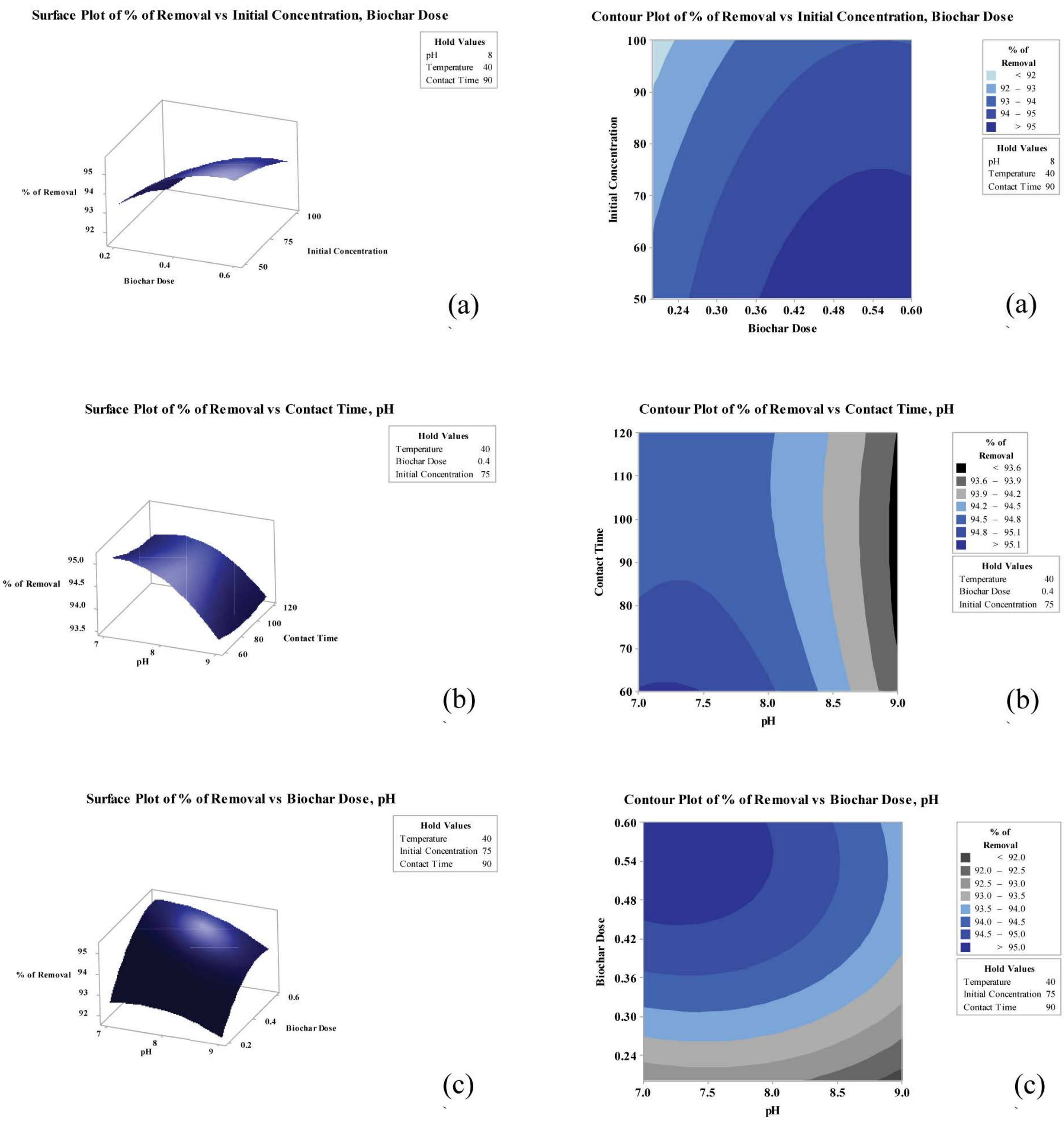

Fig. 9. Surface plots and contour plots of; % removal vs. initial concentration and biochar dosage (a), % removal vs. contact time and pH (b), % removal vs. biochar dosage and pH (c).

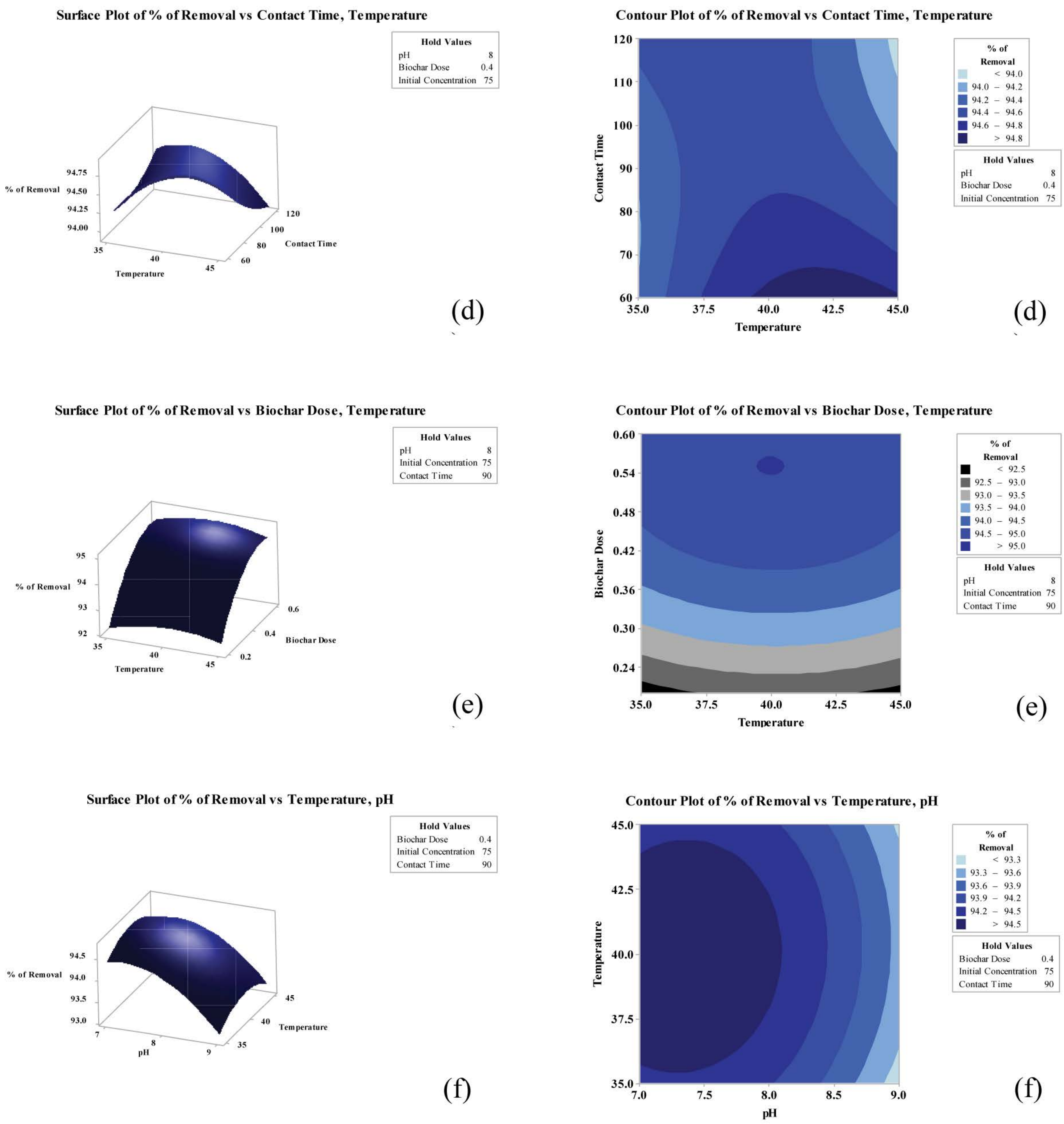

Fig. 10. Surface plots and contour plots of; % removal vs. contact time and temperature (d), % removal vs. biochar dosage and temperature (e), % removal vs. temperature and pH (f).

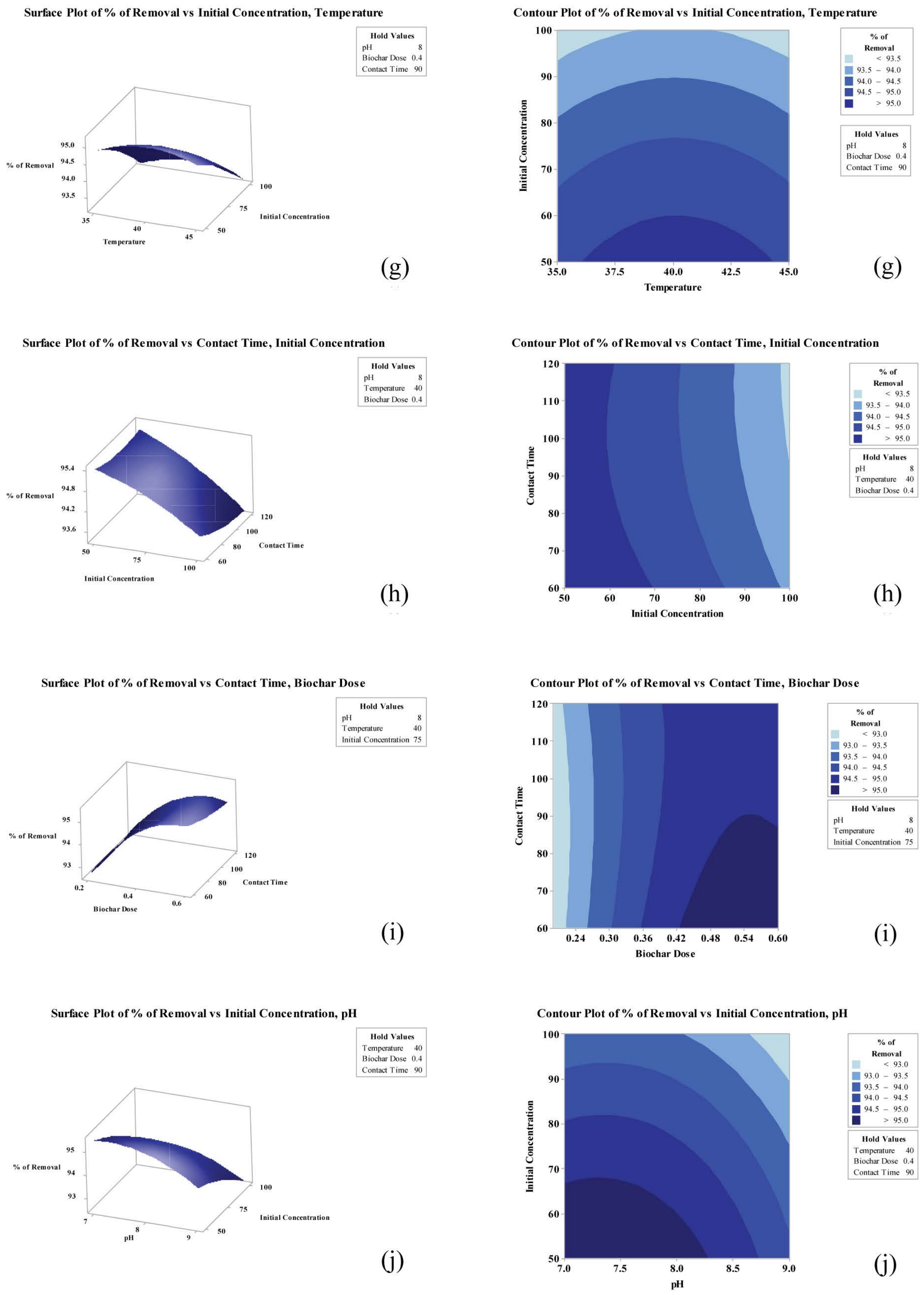

Fig. 11. Surface plots and contour plots of; % removal vs. initial concentration and temperature (g), % removal vs. contact time and initial concentration (h), % removal vs. contact time and biochar dosage (i), % removal vs. initial concentration and pH (j).

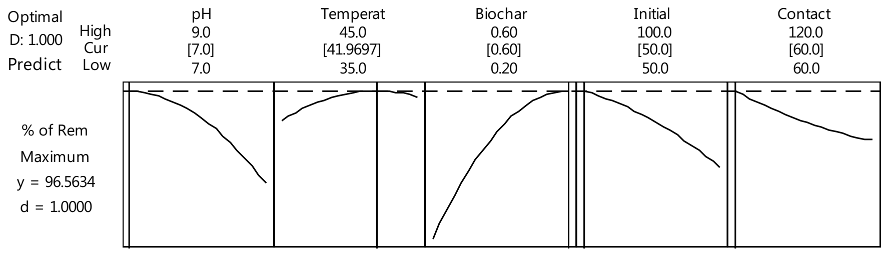

Fig. 12. Graphical representation of numerical optimization of all factors and responses.

References

[1] P. Mondal, S. Baksi, D. Bose, Study of environmental issues in textile industries and recent wastewater treatment technology, World Sci. News, 61 (2017) 98–109.

[2] E.N. El Qada, S.J. Allen, G.M. Walker, Adsorption of methylene blue onto activated carbon produced from steam activated bituminous coal: a study of equilibrium adsorption isotherm, Chem. Eng. J., 124 (2006) 103–110.

[3] M. Matsumoto, S. Usami, Photocatalytic degradation of pentachlorophenol by TiO_2 supported on mesoporous silica, Desal. Water Treat., 18 (2017) 352–356.

[4] M. El Haddad, R. Mamouni, N. Saffaj, S. Lazar, Removal of a cationic dye–Basic red 12–from aqueous solution by adsorption onto animal bone meal, J. Assoc. Arab Univ. Basic Appl. Sci., 12 (2012) 48–54.

[5] B. Kakavandi, A. Takdastan, S. Pourfadakari, M. Ahmadmoazzam, S Jorfi, Heterogeneous catalytic degradation of organic compounds using nanoscale zero-valent iron supported on kaolinite: mechanism, kinetic and feasibility studies, J. Taiwan Inst. Chem. Eng., 96 (2019) 329–340.

[6] M.A. Martin-Lara, I.L. Rodriguez Rico, I. de la Carida Aloma Vicente, G. Blazquez Garcia, M. Calero de Hoces, Modification of the sorptive characteristics of sugarcane bagasse for removing lead from aqueous solutions, Desalination, 256 (2010) 58–63.

[7] K.R. Ramakrishna, T. Viraraghavan, Dye removal using low cost adsorbents, Water Sci. Technol., 36 (1997) 189–196.

[8] Z. Aksu, Reactive dye bioaccumulation by *Saccharomyces cerevisiae*, Process Biochem., 38 (2003) 1437–1444.

[9] J. Jegan, J. Vijayaraghavan, T. Bhagavathi Pushpa, S.J. Sardhar Basha, Application of seaweeds for the removal of cationic dye from aqueous solution, Desal. Water Treat., 57 (2016) 25812–25821.

[10] T. Bhagavathi Pushpa, J. Jegan, S. Praveen, R. Gokulan, Biodecolorization of Basic blue 41 using EM based composts: isotherm and kinetics, Chemistryselect, 4 (2019) 10006–10012.

[11] A.A. Babaei, S.N. Alavi, M. Akbarifar, K. Ahmadi, A.R. Esfahani, B. Kakavandi, Experimental and modeling study on adsorption of cationic Methylene blue dye onto mesoporous biochars prepared from agrowaste, Desal. Water Treat., 57 (2016) 27199–27212.

[12] S. Rangabhashiyam, N. Selvaraju, Evaluation of the biosorption potential of a novel *Caryotaurens* inflorescence waste biomass for the removal of hexavalent chromium from aqueous solutions, J. Taiwan Inst. Chem. Eng., 47(2007) 59–70.

[13] D. Sud, G. Mahajan, M.P. Kaur, Agricultural waste material as potential adsorbent for sequestering heavy metal ions from aqueous solutions: a review, Bioresour. Technol., 99 (2008) 6017–6027.

[14] M. Omidvar Borna M. Pirsaheb, M. Vosoughi Niri, R. Khosravi Mashizie, B. Kakavandi, M. Reza Zare, A. Asadi, Batch and column studies for the adsorption of chromium(VI) on low-cost *Hibiscus Cannabinus* kenaf, a green adsorbent, J. Taiwan Inst. Chem. Eng., 68 (2016) 80–89.

[15] M. Ahmadi, M. Hazrati, B. Kakavandi, Development of maghemite nanoparticles supported on cross-linked chitosan (γ-Fe_2O_3@CS) as a recoverable mesoporous magnetic composite for effective heavy metals removal, J. Mol. Liq., 248 (2017) 184–196.

[16] M.A.P. Moreno, F.M. Agugliaro, Q.H. Escobedo, A.J.P. Moreno, Peanut shell for energy: properties and its potential to respect the environment, Sustainability, 10 (2018) 1–15.

[17] P.K. Borthakur, R.K. Bhattacharyya, U. Das, Biochar in Organic Farming, C.S. Chandran, S. Thomas, M. Unni, Eds., Organic Farming, Springer, Cham, 2019, pp. 109–134.

[18] M.S. Alam, D.S. Alessi, Chapter 4 – Modeling the Surface Chemistry of Biochars, Y.S. Ok, D.C.W. Tsang, N. Bolan, J.M. Novak, Eds., Biochar from Biomass and Waste: Fundamentals and Applications, Elsevier Radarweg 29, P.O. Box: 211, 1000 AE Amsterdam, Netherlands, 2019, pp. 59–72.

[19] R. Tareq, N. Akter, M.S. Azam, Chapter 10 – Biochars and Biochar Composites: Low-Cost Adsorbents for Environmental Remediation, Y.S. Ok, D.C.W. Tsang, N. Bolan, J.M. Novak, Eds., Biochar from Biomass and Waste-Fundamentals and Applications, Elsevier, 2019, pp. 169–209.

[20] R. Gokulan, G. Ganesh Prabhu, J. Jegan, A. Avinash, A critical insight into biomass derived biosorbent for bioremediation of dyes, Chemistryselect, 4 (2019) 9762–9775.

[21] S. Biswas, M. Bal, S.K. Behera, T.K. Sen, B.C. Meikap, Process optimization study of Zn^{2+} adsorption on biochar-alginate composite adsorbent by response surface methodology (RSM), Water, 11 (2019) 325.

[22] M.Z. Alam, S.A. Muyibi, J. Toramae, Statistical optimization of adsorption processes for removal of 2,4-dichlorophenol by activated carbon derived from oil palm empty fruit bunches, J. Environ. Sci., 19 (2007) 674–677.

[23] Z. Luo, E. Wang, H. Zheng, J.A Baldock, O.J Sun, Q. Shao, Convergent modeling of past soil organic carbon stocks but divergent projections, Biogeosci. Discuss., 12 (2015) 4373–4383.

[24] Z. Mahdi, A. El Hanandeh, Q. Yu, Date seed derived biochar for Ni(II) removal from aqueous solutions, MATEC Web Conf., 120 (2017) 05005.

[25] R. Gokulan, J. Raja Murugadoss, J. Jegan, A. Avinash, Comparative desorption studies on remediation of remazol dyes using biochar (sorbent) derived from green marine seaweeds, Chemistryselect, 4 (2019) 7437–7445.

[26] E.F. Zama, Y.G. Zhu, B.J. Reid, G.X. Sun, The role of biochar properties in influencing the sorption and desorption of Pb(II), Cd(II) and As(III) in aqueous solution, J. Cleaner Prod., 148 (2017) 127–136.

[27] S.A. Hosseini, O. Gholipoor, Removal of arsenic from aqueous solutions using $MgFe_2O_4$ nano spinel and GO/$MgFe_2O_4$ nanocomposite: an application of response surface methodology, Desal. Water Treat., 89 (2017) 162–170.

[28] G.A. Dissanayake Herath, L.S. Poh, W.J. Ng, Statistical optimization of glyphosate adsorption by biochar and activated carbon with response surface methodology, Chemosphere, 227 (2019) 533–540.

[29] K. Sen, N.K. Mondal, S. Chattoraj, J.K. Datta, Statistical optimization study of adsorption parameters for the removal of glyphosate on forest soil using the response surface methodology, Environ. Earth Sci., 76 (2017) 1–15.

[30] R. Gokulan, A. Avinash, G. Ganesh Prabhu, J. Jegan, Remediation of remazol dyes by biochar derived from *Caulerpa Scalpelliformis*–an eco-friendly approach, J. Environ. Chem. Eng., 7 (2019) 103297.

[31] J. Jegan, S. Praveen, T. Bhagavathi Pushpa, R. Gokulan, Sorption kinetics and isotherm studies of cationic dyes using groundnut (*Arachis hypogaea*) shell derived biochar a low-cost adsorbent, Appl. Ecol. Environ. Res., 18 (2020) 1925–1939.
[32] J. Jegan, S. Praveen, T. Bhagavathi Pushpa, R. Gokulan, Biodecolorization of Basic Violet 03 using biochar derived from agricultural wastes: isotherm and kinetics, J. Biobased Mater. Bioenergy, 14 (2020) 316–326.
[33] T.K. Oh, B.S. Choi, Y. Shinogi, J. Chikushi, Characterization of biochar derived from three types of biomass, bioproduction environmental sciences, J. Faculty Agric. Kyushu Univ., 57 (2012) 61–66.
[34] V. Ponnusami, V. Krithika, R. Madhuram, S.N. Srivastava, Biosorption of reactive dye using acid-treated rice husk: factorial design analysis, J. Hazard. Mater., 142 (2007) 397–403.
[35] Momina, Md. Rafatullah, S. Ismail, A. Ahmad, Optimization study for the desorption of Methylene blue dye from clay based adsorbent coating, Water, 11 (2019) 1304.
[36] S. Chakraborty, S. Chowdhury, P.D. Saha, Adsorption of Crystal violet from aqueous solution onto NaOH-modified rice husk, Carbohydr. Polym., 84 (2011) 1533–1541.
[37] S. Praveen, T. Bhagavathi Pushpa, R. Gokulan, J. Jegan, Evaluation of the adsorption capacity of *Cocos Nucifera* shell derived biochar for basic dyes sequestration from aqueous solution, Energy Sources Part A, (2020), doi: 10.1080/15567036.2020.1800142.